

Unique opto-electronic structure and photo reduction properties of sulfur doped lead chromates explaining their instability in paintings

Vanoushe Rahemi^{a,‡}, Nasrin Sarmadian^{b,‡}, Willemien Anaf^a, Koen Janssens^a, Dirk Lamoen^b, Bart Partoens^c, Karolien De Wael^{a,*}

^a AXES, Department of Chemistry, University of Antwerp, Groenenborgerlaan 171, 2020 Antwerp, Belgium.

^b EMAT, Department of Physics, University of Antwerp, Groenenborgerlaan 171, B-2020 Antwerp, Belgium.

^c CMT, Department of Physics, University of Antwerp, Groenenborgerlaan 171, B-2020 Antwerp, Belgium.

ABSTRACT: *Chrome yellow refers to a group of synthetic inorganic pigments that became popular as an artist's material from the second quarter of the 19th century. The color of the pigment, in which the chromate ion acts as a chromophore, is related to its chemical composition ($\text{PbCr}_{1-x}\text{S}_x\text{O}_4$, with $0 \leq x \leq 0.8$) and crystalline structure (monoclinic/orthorhombic). Their shades range from the yellow-orange to the paler yellow tones with increasing sulfate amount. These pigments show remarkable signs of degradation after limited time periods. Pure PbCrO_4 (crocoite in its natural form) has a deep yellow color and is relatively stable, while the co-precipitate with lead sulfate ($\text{PbCr}_{1-x}\text{S}_x\text{O}_4$) has a paler shade and seems to degrade faster. This degradation is assumed to be related to the reduction of Cr(VI) to Cr(III). We show that on increasing the sulfur(S)-content in chrome yellow, the band gap increases. Typically, when increasing the band gap, one might assume that a decrease in photo activity is the result. However, the photo activity relative to the Cr content, and thus Cr reduction, of sulfur-rich $\text{PbCr}_{1-x}\text{S}_x\text{O}_4$ is found to be much higher compared to the sulfur-poor or non-doped lead chromates. This discrepancy can be explained by the evolution of the crystal and electronic structure as function of the sulfur content: first-principles density functional theory calculations show that both the absorption coefficient and reflection coefficients of the lead chromates change as a result of the sulfate doping in such a way that the generation of electron-hole pairs under illumination relative to the total Cr content increases. These changes in the material properties explain why paler shade yellow colors of this pigment are more prone to discoloration. The electronic structure calculations also demonstrate that lead chromate and its co-precipitates are p-type semiconductors, which explains the observed reduction reaction. As understanding this phenomenon is valuable in the field of cultural heritage, this study is the first joint action of photo-electrochemical measurements and first-principles calculations to approve the higher tendency of sulfur-rich lead chromates to darken.*

Chrome yellows belong to a class of synthetic inorganic yellow-orange pigments that became popular as artists' materials from the second quarter of the 19th century; they are often encountered in masterpieces by famous painters, such as Paul Cezanne (1839-1906)¹, Vincent van Gogh (1853-1890)² and James Ensor (1860-1949)³. This pigment is also employed for industrial purposes such as painting of vehicles, airplanes, in printing inks and for colouring rubber and paper. So, it can be released into the environment through degradation and corrosion as a result of industrial use and service life of coloured products.

The chemical composition of these pigments is based on lead chromate (PbCrO_4) or co-precipitates of lead chromate and lead sulfate ($\text{PbCr}_{1-x}\text{S}_x\text{O}_4$). With increasing sulfate amount, their colour varies from yellow-orange to pale-yellow.^{4,5} From a crystallographic point of view, at room temperature, pure PbCrO_4 has a monoclinic structure,^{6,7} whereas in the $\text{PbCr}_{1-x}\text{S}_x\text{O}_4$ co-precipitates a change from monoclinic to an orthorhombic structure is observed when x exceeds 0.4.⁸⁻¹⁰ Because of their limited chemical stability, this pigment has been extensively studied by different meth-

ods such as vibrational spectroscopic and X-ray microprobe techniques.^{11,12}

In the last few years, it has been demonstrated that the darkening of chrome yellow in paintings by Vincent van Gogh is associated with the photo reduction of the lead chromate-based pigments, mainly involving the formation of Cr(III)-compounds.^{13,14} It is observed that S-rich $\text{PbCr}_{1-x}\text{S}_x\text{O}_4$ solid solutions ($x > 0.4$, with orthorhombic structure) are more prone towards photo reduction than the S-poor ones ($0 \leq x < 0.4$, with monoclinic structure). However, these observations are in contradiction with the increase in band gap (and thus expected decrease in photo activity) based on pigment colour. Some hypotheses were formulated in an attempt to explain this discrepancy. First, the greater solubility of the orthorhombic pigments has been used to explain its greater tendency for degradation, next to the type of crystal structure and the chemical composition.¹² Secondly, Munoz-Garcia et al¹⁵ recently stated that a local segregation of lead sulfate explains the degradation of the pigment. This hypothesis is based on first-principles calculations, however, it is not clear how this phenomenon of segregation might

induce the reduction or degradation of the pigment. Even more, they state that the formation of nanocomposites explains the paler hues and further ignore the S-driven band gap change which they observe. Amat et al¹⁶ performed similar calculations, however they did not observe any peculiar electronic features between monoclinic and orthorhombic series which could explain the difference in degradation behaviour.

In our work we investigate the reduction of Cr by photo-electrochemistry and show how this reduction depends on the S content. The insights gained via electrochemistry are supported by electronic structure calculations that allow us to pinpoint the relation between the reduction of Cr under illumination, the chemical instability as a function of the composition and the opto-electronic properties of the lead chromates. The suggested generic approach can be used to study semiconductor materials such as TiO₂, SnO₂ and ZnO₂ applied in e.g. solar cells.^{17,18}

Experimentally, different forms of chrome yellow were exposed to green and blue laser light (wavelengths 532 and 406 nm) while the resulting photo current was monitored. We combine photo-electrochemistry, linear sweep voltammetry, UV-vis diffuse reflectance spectroscopy and density functional theory (DFT) calculations (1) to demonstrate the formation of Cr(III) under illumination, (2) to show that the relative amount of reduced Cr (with respect to the total Cr concentration) increases with S concentration, and (3) that this can be understood from the p-like position of the band edges of the semiconductor PbCr_{1-x}S_xO₄, the exact value of the band gap, and the optical absorption spectrum, all as function of the S concentration.

Finally, the photo reduction under illumination of the full solar spectrum is considered based on DFT calculations, which supports our main conclusion that the dominating fact that S-rich PbCr_{1-x}S_xO₄ compounds are more prone to darkening is their relative increase of the reduced Cr atoms with increasing S concentration. The important role of the switch of PbCr_{1-x}S_xO₄ from the monoclinic to the orthorhombic structure in this result is stressed. The comparison between experiments and calculations in combination with other analytical techniques, spectroscopic and chromatographic analysis, opens up new perspectives in the field of pigment degradation studies through a better understanding of the alteration mechanisms taking place.

Experimental

Graphite working electrodes ($\varnothing = 3$ mm) were pretreated by mechanical polishing with a P400 SiC-paper in order to obtain a rough surface. To remove any adherent SiC-particles, the electrodes were rinsed with deionized water in an ultrasonic bath for 20 seconds. For the electrochemical setup exploring the semiconductor properties,^{19,20} powders of monoclinic PbCrO₄ (Sigma-Aldrich) and in-house synthesized PbCr_{1-x}S_xO₄ containing a variable sulfate content ($0.1 \leq x \leq 0.8$) were used for the graphite|pigment working electrode preparation. The procedure of synthesis of the PbCr_{1-x}S_xO₄ pigments is reported elsewhere.¹² An amount of 1.50 μ L of either ethanol-PbCrO₄ or ethanol-PbCr_{1-x}S_xO₄ suspension was dripped onto the electrode. After solvent evaporation, a thin layer of the respective pigment is left at

the electrode surface. The modified electrodes are denoted as C|PbCrO₄ and C|PbCr_{1-x}S_xO₄. A saturated calomel electrode (SCE) and a platinum (Pt) electrode were used as the reference (RE) and counter electrode (CE), respectively. The working electrode (WE) with the pigment side oriented upward was positioned in an open container. The latter was filled with 4 mL solution of electrolyte (1 mM NaCl solution or the non-aqueous ionic liquid (IL) 1-butyl-3-methylimidazolium tetrafluoroborate ([BMIM][BF₄])) involving alternating cycles of darkness (~ 10 s) and illumination (~ 10 s) using a 406 nm blue laser at 30 mW power or a 532 nm green laser at 30 mW power. Solutions were purged by pure nitrogen prior to the experiment and maintained under nitrogen atmosphere during measurements. Electrochemical measurements were performed by an Autolab PGSTAT101 potentiostat (Metrohm, the Netherlands) with NOVA 1.10 software. The photo currents that spontaneously starts running between the working electrode and the counter electrode upon laser irradiation of the pigment is measured. This current is considered to be a measure for the photo activity of the pigments and allows to experimentally compare the photo activity between different lead chromates in a fast and efficient manner.

Diffuse reflectance UV-vis spectroscopic (DR-UV-vis) measurements of lead chromate were obtained by means of an Evolution 500 UV-vis double beam spectrophotometer equipped with a DR-UV integrated sphere, Thermo Electron Corporation, Waltham, Massachusetts. The pigment powders were mixed and crushed with KBr dried at 200°C (0.02 g of PbCrO₄ in 0.98 g of KBr). The mixtures were homogeneous and positioned in the DR-UV-vis cell for measuring in the 250-800 nm range.

Computational

Density functional theory (DFT)^{21,22} calculations were performed using the plane-wave basis set and the projector augmented-wave method,²³ as implemented in the Vienna Ab-initio Simulation Package (VASP).²⁴⁻²⁷ We used DFT+U^{28,29} and the Perdew-Burke-Ernzerhof (PBE) exchange and correlation functional^{30,31} to calculate the lattice parameters of various lead chromate materials and relax the atomic positions, as well as to determine their electronic structure and optical properties. A Hubbard U parameter of 3.7 eV was used for the Cr atoms.³² We used an energy cutoff of 400 eV for the plane-wave basis set. To sample the Brillouin zone, we used a 6 \times 4 \times 4 Monkhorst-Pack (MP) grid³³ making sure that the Γ point was included in the mesh. Note that atomic relaxations were made until residual forces on the atoms are less than 0.01 eV/Å and total energies converged to within 1 meV.

The effects of S-doping on the opto-electronic properties of PbCrO₄ (PbCr_{1-x}S_xO₄ with $x = 0, 0.1, 0.25, 0.5, 0.75, 0.8$ and 1) were studied by using a 96-atom supercell, consisting of 3 \times 1 \times 1 conventional cells. For each S-concentration, two structures (monoclinic and orthorhombic) were considered. Our calculations showed that for a S-concentration below 50%, the monoclinic structure is the ground state. Starting from 50%, the orthorhombic structure becomes the most stable structure. The calculated results are consistent with the experimental ones that indicate the monoclinic (orthorhom-

bic) structure to be the ground state of $\text{PbCr}_{1-x}\text{S}_x\text{O}_4$ for an S-content below (above) 40%.⁶⁻¹⁰ In what follows, we always present the results of the most stable structure of the studied compounds.

In order to study the changes in the energy positions of the valence and conduction band due to the S-doping, the branch point energy (BPE) was calculated as a weighted average of the midgap energies over the Brillouin zone,³⁴

$$\text{BPE} = \frac{1}{2N_k} \sum_{\mathbf{k}} \left[\frac{1}{N_{\text{CB}}} \sum_i^{N_{\text{CB}}} \varepsilon_{\text{ci}}(\mathbf{k}) + \frac{1}{N_{\text{VB}}} \sum_j^{N_{\text{VB}}} \varepsilon_{\text{vj}}(\mathbf{k}) \right]$$

Here, N_k is the number of points in the k-point mesh, N_{CB} and N_{VB} are the number of conduction and valence bands considered for the averaging, with ε_{ci} and ε_{vj} their corresponding energies. The number of valence and conduction bands used was determined according to the number of valence electrons in the cell, as explained in the work of Schleife et al.³⁵.

In order to calculate the photo absorption current induced in the various materials under illumination, we first calculated their optical properties (excitonic effects were neglected). The imaginary part of the dielectric function is obtained within the random phase approximation. The real part then follows from the Kramers-Kronig relation. For each doping concentration, we averaged the dielectric function with respect to the direction of polarization. We found that it was sufficient to sample the Brillouin zone using a $12 \times 8 \times 8$ MP grid for our supercell in order to obtain a converged dielectric function. We included four times the number of occupied bands as total number of bands in the dielectric function calculations to guarantee a converged dielectric function in the 0–45 eV energy range.

Results and Discussion

Photo activity of lead chromate

Bandiello et al.³⁶ and Errandonea et al.³⁷ consider PbCrO_4 to be a semiconductor with a direct band gap of 2.3 eV, a value consistent with the yellow colour of the pigment. The colour of chrome yellow pigments originates from the absorption of light, giving rise to excitation of an electron from the valence band (VB) to the conduction band (CB). The inset in Figure 1 shows that oxidative photo currents are observed when PbCrO_4 , in contact with an aqueous NaCl solution, is illuminated with blue laser light. The sign of the current indicates that electrons move externally from the WE to the CE, and thus that an oxidation occurs at the WE. Since chromium in CrO_4^{2-} is in its highest oxidation state (+VI), no further oxidation is expected. Therefore, we assume that the oxidation of water in the NaCl solution takes place and thus that the potential φ^{ox} is estimated to lie below the oxidation potential of water. Thus, in an aqueous environment and upon illumination with an energy larger than the band gap, CrO_4^{2-} is stable against oxidation.

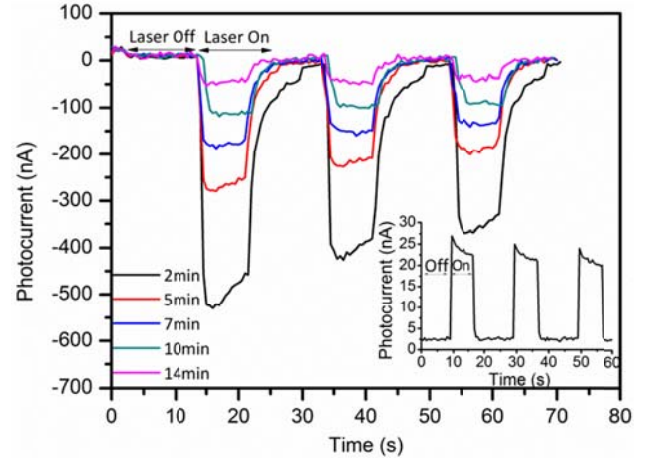


Figure 1. Photo-electrochemical response of a $\text{C}|\text{PbCrO}_4$ electrode, irradiated with a 406 nm blue laser, after 10 s of illuminations. Main figure: $\text{C}|\text{PbCrO}_4$ electrode in contact with the ionic liquid. Inset: $\text{C}|\text{PbCrO}_4$ electrode in contact with NaCl solution.

To confirm this hypothesis, the ionic liquid $[\text{BMIM}][\text{BF}_4]$ was used to replace the aqueous electrolyte. The latter has a significantly higher resistance to electrochemical redox phenomena due to its large electrochemical window of stability (of around 6 V).³⁸ As shown by the black curve in Figure 1, the ionic liquid (IL) induces a clear reduction current upon illumination by blue light, i.e. a current that is opposite in direction to what is observed for the NaCl solution. The average current of the illuminated PbCrO_4 in the IL can reach ca 500 nA. In contrast, the current measured in darkness remains below 3 nA. After prolonged irradiation (up to 15 min), a gradual decrease in photo current is observed. Since the IL cannot participate either in oxidation or reduction half-reactions, our interpretation is that CrO_4^{2-} itself is reduced during the illumination in these conditions, and thus that the reduction potential φ^{red} of Cr lies below the conduction band minimum (CBM) of PbCrO_4 . The redox potentials of PbCrO_4 relative to the CBM of PbCrO_4 and the oxidation potential of water as they are deduced from these experiments are schematically shown in Figure 2. Further the scheme is extended with the reduction potential of water which is 0.25 eV above the Cr reduction potential based on the Pourbaix diagram.³⁷ The relative energy difference of these redox potentials with the CBM and valence band maximum (VBM) are estimated based on the calculations discussed later. To summarize, Figure 3 also illustrates our interpretation of the experiments in terms of the dominating redox reactions at the WE in case of illumination of lead chromate. While the oxidation of water occurs in case of the aqueous NaCl solution, the current changes sign in the IL solution resulting in the reduction of Cr at the WE. Therefore we call the measured photo current in the presence of the IL a photo reduction current.

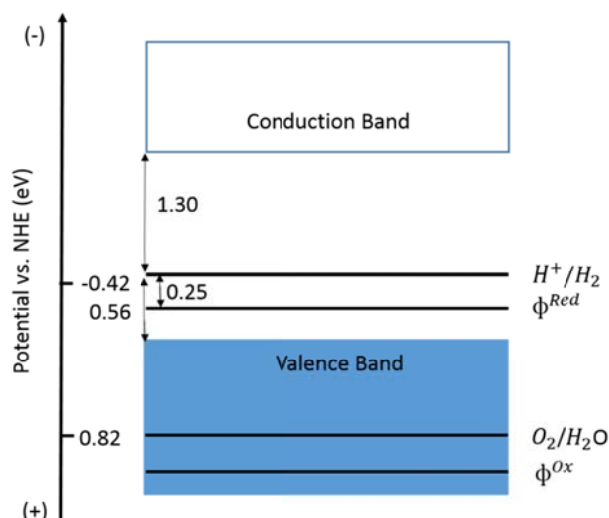


Figure 2. Oxidation and reduction potentials of PbCrO_4 relative to the redox potential of water (for pH 7).

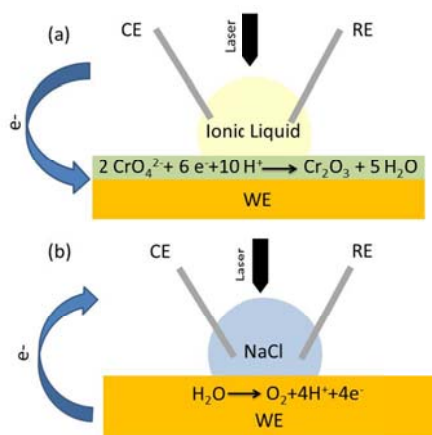


Figure 3. Schematic overview on the electron flow between working electrode (covered with PbCrO_4) and counter electrode (a) in an ionic liquid and (b) in aqueous NaCl solution. The green colour indicates the formation of Cr_2O_3 when the experiments are performed in an ionic liquid.^{11-14,39}

During a long-term illumination experiment in $[\text{BMIM}][\text{BF}_4]$, the photo current was recorded at fixed time intervals of 1 to 15 minutes. As shown in Figure 1, a gradual decrease of the photo reduction current took place. This may be explained as being caused by a gradual CrO_4^{2-} degradation, involving its replacement at the electrode surface by Cr(III) compounds.

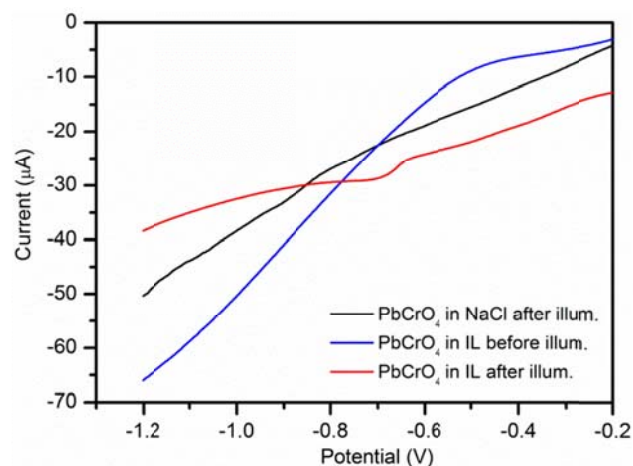


Figure 4. Linear sweep voltammetry (LSV) in the -0.2 to -1.2 V range confirms the presence of Cr(III) at surface of the PbCrO_4 electrode after illumination in an ionic liquid.

In Figure 4, results of linear sweep voltammetry (LSV) for C|PbCrO_4 are shown from -0.20 to -1.20 V in both 1 mM NaCl and IL. When immersed in NaCl, no photo reduction is observed. In IL, but only after illumination, a reduction process is apparent at -0.71 V, corresponding to the formation of Cr(III) at the C|PbCrO_4 electrode.⁴⁰ Without illumination, no Cr(III) is apparent.

All these experiments suggest that PbCrO_4 is a p-type semiconductor, because i) in a p-type semiconductor the conduction band minimum (CBM) is more likely to be above the reduction potential, and ii) a downwards band bending is expected at the interface of the p-type semiconductor and the electrolyte, causing the electrons to move towards the interface as experimentally observed. Note that also the larger magnitude of the current in case of the IL might be attributed to the fact that electrons at the CBM have a smaller effective mass than holes at the VBM.

However, beside their thermodynamics the kinetics of the half-cell reactions is important to identify which half-reaction dominates at the semiconductor-electrolyte interface, which probably explains why the sign of the observed photo current reverses again if a small amount of aqueous NaCl is added to the IL, as shown in Figure S1.

In the previous section, only the monoclinic PbCrO_4 pigment powder was examined by using electrochemistry. Monaco et al.¹² observed a more pronounced darkening tendency upon illumination of lead chromate-lead sulfate coprecipitates ($\text{PbCr}_{1-x}\text{S}_x\text{O}_4$, $0 < x < 0.8$) with increasing x . Therefore, we performed similar electrochemical experiments for $\text{PbCr}_{1-x}\text{S}_x\text{O}_4$ coprecipitates ($0.1 \leq x \leq 0.8$). In Figure S2 the photo-electrochemical response under the blue laser illumination of various electrodes modified with $\text{PbCr}_{1-x}\text{S}_x\text{O}_4$ coprecipitates ($0.1 \leq x \leq 0.8$), immersed in an IL and a NaCl solution, are compared. All investigated $\text{PbCr}_{1-x}\text{S}_x\text{O}_4$ coprecipitates show the same behaviour as PbCrO_4 : photo activation in all cases leads to oxidation of the environment in a NaCl solution and to a reduction of CrO_4^{2-} in presence of the IL. These observations are linked to the p-type semiconductor properties of $\text{PbCr}_{1-x}\text{S}_x\text{O}_4$ and the reduction of Cr(VI)

□

to Cr(III) in the IL. Thus for all these compounds, it is expected that the Cr reduction potential stays below the CBM. As all the pigments on the WE are prepared in the same way and thus the amount of pigment is the same, the absolute values of the currents can also be compared. Note from Figure S2 that this absolute value of the photo reduction current decreases with increasing S concentration. However, Figure 5 shows this current (averaged over the first illumination interval) relative per Cr atom. This observation indicates that, relative to the total number of Cr atoms, more Cr atoms are reduced if the S concentration increases. We believe that this is the key observation to understand why S-rich $\text{PbCr}_{1-x}\text{S}_x\text{O}_4$ is more prone to darkening than PbCrO_4 . The aim of our first-principles calculations is to support this interpretation of the experimental measurements. Therefore we first address the overall electronic properties of $\text{PbCr}_{1-x}\text{S}_x\text{O}_4$ as function of S concentration x .

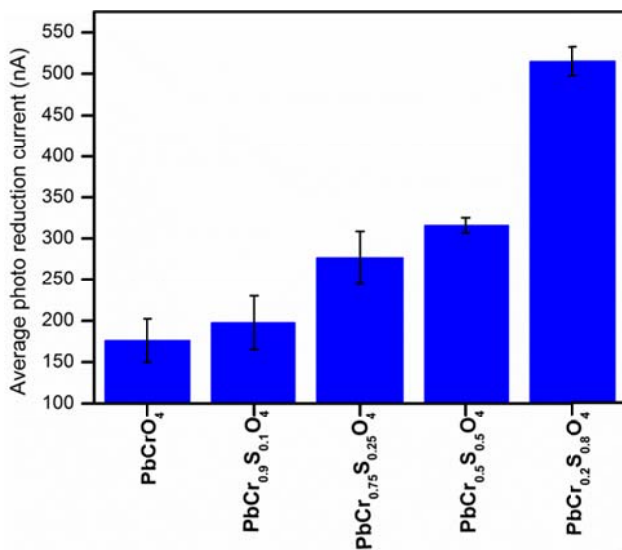


Figure 5. Comparison of the monitored photo reduction current via electrochemistry of lead chromate and the other co-precipitates under blue laser illumination (wavelength 406 nm). The experimental photo reduction current is normalized with respect to the Cr-content of the corresponding pigment materials.

Electronic structure of lead chromate and co-precipitates $\text{PbCr}_{1-x}\text{S}_x\text{O}_4$

The diffuse reflectance UV-vis spectrophotometry spectra of the investigated series of chrome yellows show a typical shape for a photoactive, semiconducting material, exhibiting a clear absorption edge (see Figure 6). From the extrapolated tangent of the most vertical part of the edge, the corresponding absorption wavelength was deduced, and subsequently converted to the band gap energy. Powders of PbCrO_4 , $\text{PbCr}_{0.9}\text{S}_{0.1}\text{O}_4$, $\text{PbCr}_{0.75}\text{S}_{0.25}\text{O}_4$, and $\text{PbCr}_{0.2}\text{S}_{0.8}\text{O}_4$ show a band gap energy of 2.20, 2.22, 2.25 and 2.33 eV, respectively, i.e. an increasing trend is clearly observed.

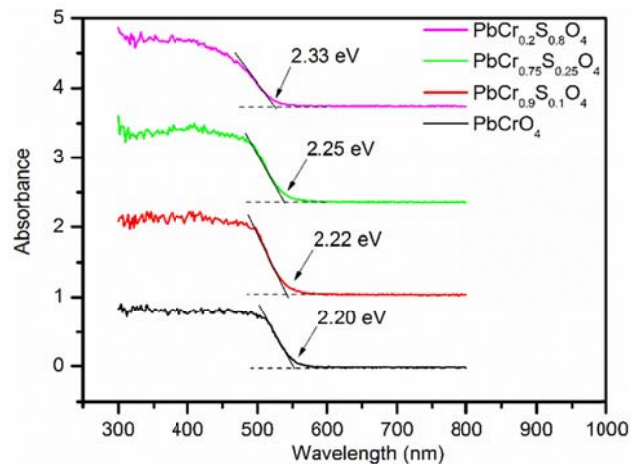


Figure 6. UV-DR measurements of PbCrO_4 , $\text{PbCr}_{0.9}\text{S}_{0.1}\text{O}_4$, $\text{PbCr}_{0.75}\text{S}_{0.25}\text{O}_4$, and $\text{PbCr}_{0.2}\text{S}_{0.8}\text{O}_4$. The corresponding band gap energies are indicated.

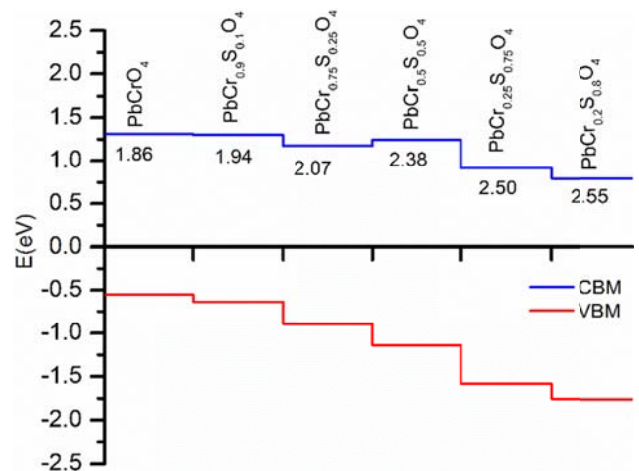


Figure 7. Valence and conduction band energies with respect to the BPE. The value of the band gap is also presented.

In Figure 7 we plot the relative positions (with respect to the BPE) of the CBM and the VBM of $\text{PbCr}_{1-x}\text{S}_x\text{O}_4$ for various values of x as calculated within DFT. Also the obtained band gaps are indicated. In comparison with PbCrO_4 , $\text{PbCr}_{0.2}\text{S}_{0.8}\text{O}_4$ shows a downward shift of the VBM by 1.25 eV that is accompanied by a small downward shift of the CBM, resulting in a net increase of the band gap by 0.69 eV. One can observe that, with increasing S concentration, the band gap increases, and that this increase is mainly due to a decrease of the VBM position. In previous work^{41, 42} we have shown that compounds for which the BPE falls in the VB or in the lower part of the band gap should be considered as p-type semiconductors. It is therefore clear from Figure 7 that our calculations support this claim which was based on the interpretation of the experimental results: the predicted typical p-type position of the band edges of PbCrO_4 confirms the tendency towards photo reduction of this pigment. Furthermore, because upon increasing the S-content mainly the VBM shifts downwards, the reduction potential of Cr will stay located below the CBM, favouring the photo reduction also for the co-precipitates including S, again as observed experimental-

□

ly. If we use the position of the branch point energy obtained with Schleife's rule as a very rough estimate of the reduction potential of water,⁴² we obtain the schematic lay-out of the relative positions of the different redox potentials and the position of the CBM and VBM in Figure 2.

It is also instructive to investigate the evolution of the electronic structure with changing S concentration as it will have a direct influence on the photo absorption. Figure 8 shows the projected DOS for the different studied compounds. The reduced band width of the conduction band (CB) and the gradual disappearance of the two first CB blocks in the unoccupied DOS are a direct consequence of the gradual replacement of Cr by S atoms. For PbSO_4 , the Pb 3s orbitals comprise the CB. Figure 8 shows also that the VB is made up mainly of O 2p orbitals while Cr 3d orbitals are the main contributors to the CB of $\text{PbCr}_{1-x}\text{S}_x\text{O}_4$.

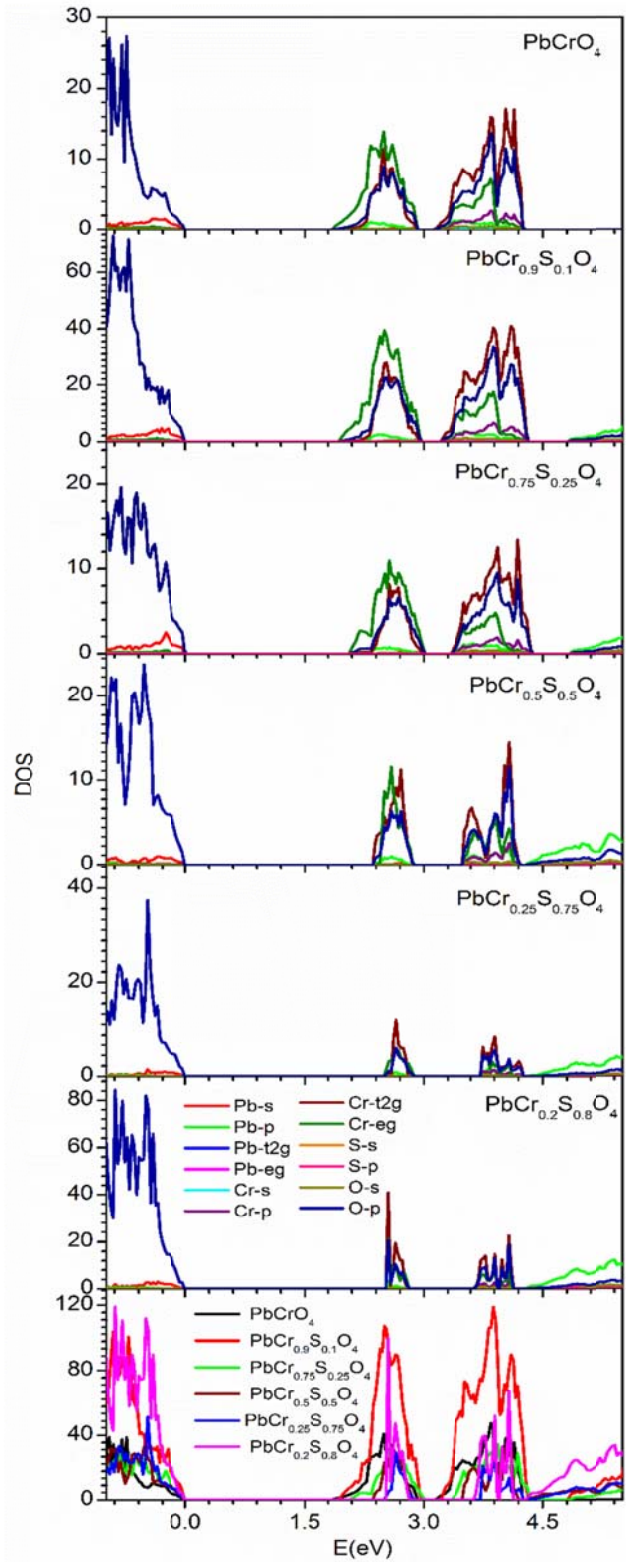


Figure 8. Density of states (DOS) for $\text{PbCr}_{1-x}\text{S}_x\text{O}_4$. The lower panel compares the total DOS of $\text{PbCr}_{1-x}\text{S}_x\text{O}_4$ for all values of x . The energy range is the same in all figures.

□

Optical properties and photo absorption current

Assuming that the photo-generated electron-hole pairs are responsible for the measured photo reduction current we study the generation of electron-hole pairs due to the absorption of light and its trend as a function of S-content. Using the imaginary and real part of the dielectric function $\sqrt{\epsilon} = n + i\kappa$, the absorption coefficient of the materials was calculated as $\alpha = 2\omega\kappa/c$ where ω , c , n ($= \sqrt{\frac{\epsilon_i^2 + \epsilon_r^2 + \epsilon_r}{2}}$), and κ ($= \sqrt{\frac{\epsilon_i^2 + \epsilon_r^2 - \epsilon_r}{2}}$) are the frequency, speed of light, refractive index, and extinction coefficient of the material, respectively. The fraction of the light absorbed in a partially reflecting film layer of thickness L is modelled as

$$I_{ph} = a I_0 = (1 - R)(1 - e^{-\alpha L}) I_0$$

where R is the reflectance of the layer. R is calculated using the Fresnel s for normal light incidence:

$$R = \frac{[(n-1)^2 + \kappa^2]}{[(n+1)^2 + \kappa^2]}$$

I_0 is the intensity of the impinging light, a is the absorbance. We call I_{ph} the photo absorption current.

Figure 9 shows the calculated absorbance. The typical size of the pigment crystallites was chosen as the thickness of $L = 3 \mu\text{m}$, although our conclusions do not depend on this choice. The change in the optical properties of the pigments is directly correlated with the altering orbital character of the CB. The intensity of the onset of the imaginary part of the dielectric function (ϵ_i) decreases when replacing Cr by S due to the reduction of available states in the CB (see also Figure 8). A concomitant increase of the onset energy is observed in ϵ_i (see Figure S3, which shows the imaginary part of the dielectric function for different S concentrations). This leads to a systematic blue shift in the optical band gap and the absorbance of $\text{PbCr}_{1-x}\text{S}_x\text{O}_4$ on replacing Cr by S as shown in Figure 9.

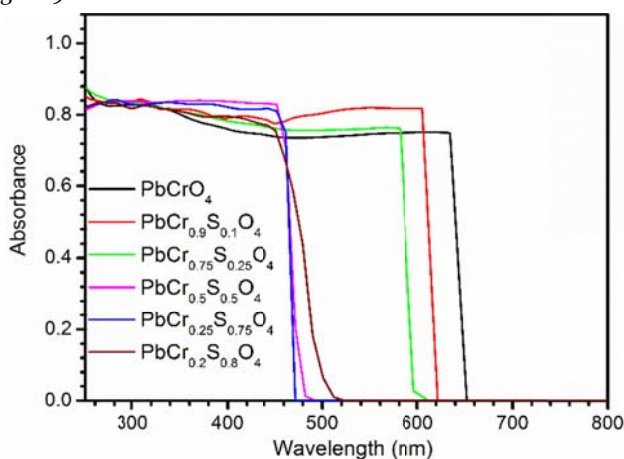


Figure 9. Calculated absorbed fraction a of the impinging light intensity as a function of the wavelength for a film thickness $L = 3 \mu\text{m}$.

We will now show that there is indeed a direct link between this photo absorption current and the measured photo

reduction current. Therefore we calculated how much smaller or larger the photo current of $\text{PbCr}_{1-x}\text{S}_x\text{O}_4$ is relative to the one of PbCrO_4 :

$$\frac{I_{ph}(\text{PbCr}_{1-x}\text{S}_x\text{O}_4)}{I_{ph}(\text{PbCrO}_4)} = \frac{[1 - R(x)][1 - \exp(-\alpha(x)L)]}{[1 - R(0)][1 - \exp(-\alpha(0)L)][1 - x]}$$

The $1/(1-x)$ factor indicates the scaling per Cr atom. In Figure 10, this ratio is shown for illumination under 406 nm blue light and compared to the ratio of the experimentally measured photo reduction currents of $\text{PbCr}_{1-x}\text{S}_x\text{O}_4$ and PbCrO_4 for different values of x , as deduced from the experimental data shown in Figure 5. The corresponding absorption (α) and reflectivity (R) coefficients of the pigments are shown in the inset. With increasing S concentration x , the decrease in absorption is accompanied by a decrease in the reflectivity of the material, resulting in a net increase of the photo absorption current. Both measurements and calculations show qualitatively a similar, positive trend vs increasing S concentration x . However, there is a considerable difference between the measured photo reduction current ratio and the calculated photo current ratio for $\text{PbCr}_{0.2}\text{S}_{0.8}\text{O}_4$: experimentally an increase in photo current by a factor of 2.4 is observed while the calculations predict an almost 5-fold increase. This difference may be attributed to the fact that the calculated photo absorption current includes all created electron-hole pairs, while only part of them will lead to the reduction of a Cr atom. Electron-hole recombination processes are not included in the calculation model. Furthermore, the rates of these recombination processes will depend on the S concentration.

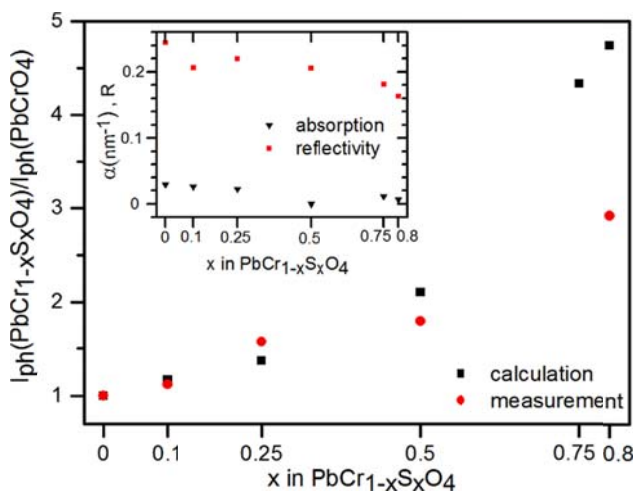


Figure 10. The ratio's of the calculated photo absorption currents and the measured photo reduction currents of $\text{PbCr}_{1-x}\text{S}_x\text{O}_4$ to that of PbCrO_4 for $\text{PbCr}_{1-x}\text{S}_x\text{O}_4$ pigments illuminated with a blue laser ($\lambda = 406 \text{ nm}$), scaled per Cr atom. The inset shows the calculated absorption (black) and reflectivity (red) constants of the materials at $\lambda = 406 \text{ nm}$.

Compelling experimental evidence to support our findings was given by green laser ($\lambda = 532 \text{ nm}$) experiments and calculations. Figure 11 shows that when PbCrO_4 and $\text{PbCr}_{1-x}\text{S}_x\text{O}_4$ ($0 \leq x \leq 0.8$) are exposed to a green laser, the photo-electrochemical response of the various $\text{PbCr}_{1-x}\text{S}_x\text{O}_4$ coprecipitates ($0 \leq x \leq 0.25$) slightly increases with increasing S-content. A marked decrease in photo reduction current is

□

observed when the relative amount of S exceeds 25% ($x > 0.25$). This can be understood by considering the band gap of these compounds in relation to the green laser wavelength employed for the excitation. This is consistent with the calculated results for the absorbance shown in Figure 9: for $x > 0.25$, the absorbance is reduced at 532 nm.

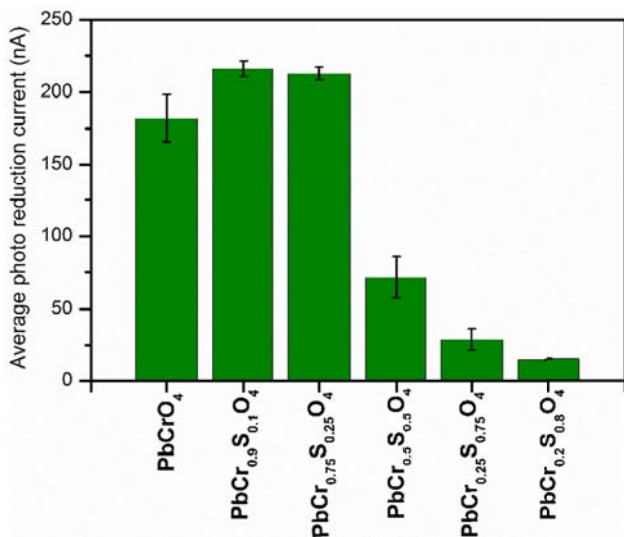


Figure 11. Comparison of the monitored photo reduction current via electrochemistry of lead chromate and the other co-precipitates under green laser illumination (wavelength 532 nm).

In Figure 12 the experimental photo reduction current and the calculated photo absorption current are compared for the illumination under green laser light. Again good agreement between the experimental and theoretical results is obtained. Figure 12 is consistent with Figure 9 and confirms that the excitation of the electrons using a green laser is theoretically not possible for the pigments with $x \geq 0.5$. As the green laser light is not powerful enough to excite electrons from valence to conduction band for these pigments, we do not expect a contribution to the photocurrent explaining the zero values for the calculated currents. However, for $x = 0.5, 0.75$ and 0.8 we observe a noticeable but lower value for the photocurrent compared to the photocurrent recorded for pigments with $x < 0.5$ (showing absorbance, monoclinic in nature). For $x = 0.5$, we are at the transition phase between monoclinic-orthorhombic which might explain a higher contribution to the recorded photocurrent compared to $x = 0.75$ and 0.8 , which are both orthorhombic species. Next to the fact that the dark current always contributes to the recorded current in the electrochemical experiments, it was observed by Monico et al.⁴³ that the presence of intermediate species such as Cr(V) under green laser light might result in an absorption feature at this spectral range and thus leading to a contribution to the photocurrent for pigments with $x \geq 0.5$.

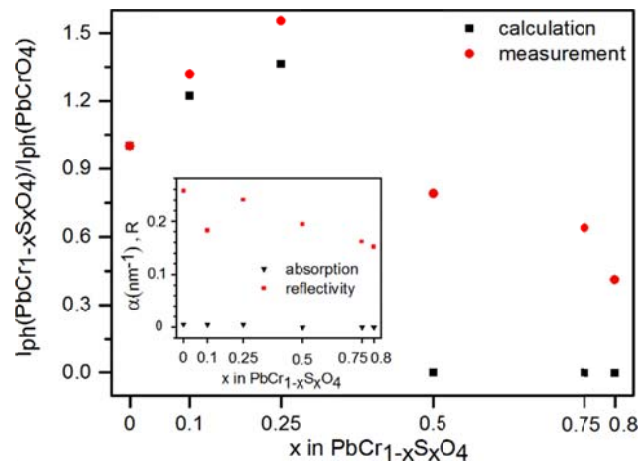


Figure 12. The ratio's of the calculated photo absorption currents and measured photo reduction currents of PbCr_{1-x}S_xO₄ to that of PbCrO₄ for PbCr_{1-x}S_xO₄ pigments illuminated with a green laser ($\lambda = 532$ nm). The inset shows the calculated absorption and reflectivity absorption (black) and reflectivity (red) constants of the materials at $\lambda = 532$ nm.

Photo reduction under solar light illumination

Our calculations thus support the experimental claim that the measured current is due to the reduction of Cr and that there is a direct link between this measured photo reduction current and the generated electron-hole pairs under illumination, i.e. the calculated photo absorption current. The calculated increase in photo absorption current with S concentration under illumination with blue light, and relative to the number of Cr atoms, is also in agreement with the experimental claim that, per Cr atom, more Cr atoms are reduced with increasing S concentration. As this conclusion is only based on illumination under a single blue wavelength, it is not possible yet to state that PbCr_{1-x}S_xO₄ pigments are more prone to darkening for large S concentration, because it goes along with an increase in the number of reduced Cr atoms. This darkening occurs under illumination with light containing all frequencies present in the solar light. And as the experiment with the green light indicates, the reduction of Cr diminishes for large wavelengths due to the increase in band gap with increasing S content. It means that the degradation behaviour of the pigments might be different under the full solar spectrum. Therefore we calculated the photocurrent of the pigments under the illumination of the solar light in the wavelength range of 280 to 3400 nm (UV-NIR) using

$$I_{ph} = \int_{280}^{3400} a(\lambda) I_0(\lambda) d\lambda / \int_{280}^{3400} I_0(\lambda) d\lambda$$

where $a(\lambda)$ is the wavelength dependent absorbance of the pigment and $I_0(\lambda)$ is the intensity of the impinging solar light AMG1.5. Thus for each wavelength the intensity of the light received at the earth surface is taken into account.⁴⁴

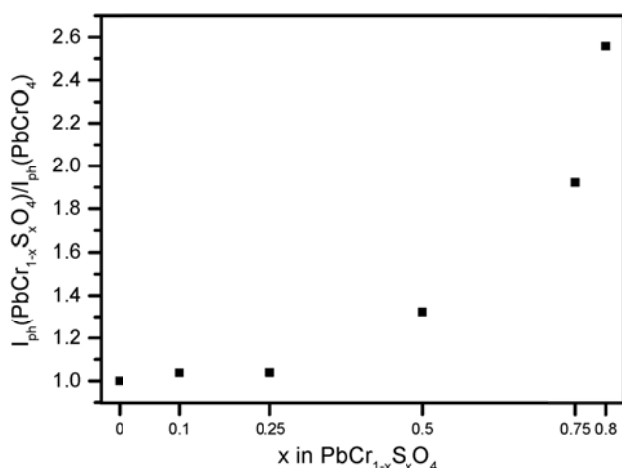


Figure 13. The ratio's of the photo absorption currents of $\text{PbCr}_{1-x}\text{S}_x\text{O}_4$ to that of PbCrO_4 for $\text{PbCr}_{1-x}\text{S}_x\text{O}_4$ pigments illuminated with solar light ($280 < \lambda < 3400$ nm).

The ratio of this photo absorption current, relative to lead chromate and per Cr atom, is shown in Figure 13. We see that, although the band gap increases with S concentration, the calculated photo absorption current per Cr atom still increases. Consequently, we predict that also the photo reduction current shows this behaviour, i.e. an increase of the photo reduction current of lead chromate co-precipitates $\text{PbCr}_{1-x}\text{S}_x\text{O}_4$ pigments with increasing S content. We also stress that we find that this increase in photo absorption current only occurs because $\text{PbCr}_{1-x}\text{S}_x\text{O}_4$ turns into the orthorhombic structure for $x \geq 0.5$. For the monoclinic phase, this increase is not observed, as shown in Figure S4 of the supplementary material.

Conclusion

To conclude, experimental techniques and DFT calculations demonstrate the formation of Cr(III) under illumination and clearly indicate that the relative amount of reduced Cr increases with S concentration. The p-type position of the band edges and the unique optical absorption spectrum are responsible for this phenomenon. The calculations support the reduction of Cr due to a position of the conduction band minimum for lead chromate and its co-precipitates $\text{PbCr}_{1-x}\text{S}_x\text{O}_4$ above the ϕ_{red} . By illumination of lead chromates by blue laser light, it is shown experimentally that this Cr reduction increases with S-content, with respect to the total Cr-content in the pigment, consistent with the increase of the calculated photoabsorption current with increasing S-content. Conclusive proof was given by the green laser experiments and calculations. A decrease in absorbance at 532 nm explains the decrease in photoreduction current for pigments with $x \geq 0.5$, also linked to the crystalline structure of the pigment. When illumination under the full solar spectrum was taken into account in the calculation, the scaled photoabsorption current was still found to increase with increasing S-content because $\text{PbCr}_{1-x}\text{S}_x\text{O}_4$ turns into the orthorhombic structure for high S-content. This critical comparison between experiments and calculations opens up new perspectives in the field of pigment degradation studies through a

better understanding of the alteration mechanisms that are taking place.

ASSOCIATED CONTENT

Supporting Information

Photo current changes subsequently in an aqueous 0.001 M NaCl solution, a 1:1 mixture of 0.001 M NaCl and Ionic Liquid, and Ionic Liquid; photo reduction current of $\text{PbCr}_{0.9}\text{S}_{0.1}\text{O}_4$, $\text{PbCr}_{0.75}\text{S}_{0.25}\text{O}_4$ and $\text{PbCr}_{0.2}\text{S}_{0.8}\text{O}_4$ in IL; calculated imaginary part; The ratio's of the photo absorption currents of $\text{PbCr}_{1-x}\text{S}_x\text{O}_4$ to that of PbCrO_4 for $\text{PbCr}_{1-x}\text{S}_x\text{O}_4$ pigments illuminated with solar light. This material is available free of charge via the Internet at <http://pubs.acs.org>.

AUTHOR INFORMATION

Corresponding Author

* Karolien De Wael, karolien.dewael@uantwerpen.be

Author Contributions

V.R. performed the measurements. N.S. performed the simulations; V.R., N.S, W.A. and K.J. wrote the manuscript; B.P., D.L. and K.D.W. coordinated the work; all authors reviewed and commented on the experiments and manuscript. ‡These authors contributed equally.

Funding Sources

The BOF-GOA action SOLARPAINT of the University of Antwerp Research Council is acknowledged for financial support. W.A. acknowledges support from BELSPO project S2-ART.

ACKNOWLEDGMENT

The computational resources and services used in this work were provided by the VSC (Flemish Supercomputer Center) and the HPC infrastructure of the University of Antwerp (CalcUA), both funded by the Hercules Foundation and the Flemish Government - department EWI. The BOF-GOA action SOLARPAINT of the University of Antwerp Research Council is acknowledged for financial support. W.A. acknowledges support from BELSPO project S2-ART. Dr. L. Monico and Dr. C. Miliani (ISTM, Perugia) are gratefully acknowledged for helpful discussions and for providing some of the initial batches of the materials studied.

REFERENCES

- (1) Butler, M. H. *J. Am. Inst. Conserv.* **1973**, *13*, 77-85.
- (2) van Gogh, V.; van Heugten, S.; Pissarro, J.; Stolwijk, C.; Bruin, G.; van Dijk, M.; Field, J.; Art, M. o. M.; Van Gogh Museum, A. *Van Gogh and the Colors of the Night*; The Museum of Modern Art, New York, 2008.
- (3) Snickt, G. V. d.; Janssens, K.; Schalm, O.; Aibéo, C.; Kloust, H.; Alfeld, M. *X-Ray Spectrom.* **2010**, *39*, 103-111.

(4) Feller, R. L.; Roy, A. *Artists' Pigments: A Handbook of Their History and Characteristics*; National Gallery of Art, Washington, 1986.

(5) Eastaugh, N.; Walsh, V.; Chaplin, T.; Siddall, R. *Pigment Compendium: A Dictionary of Historical Pigments*; Elsevier Science, Amsterdam, 2004.

(6) Korenberg, C. *British Museum Technical Research Bulletin* **2008**, *2*, 49-57.

(7) Effenberger, H.; Pertlik, F. In *Zeitschrift für Kristallographie - Crystalline Materials* **1986**, *176*, 75-83.

(8) Crane, M. J.; Leverett, P.; Shaddick, L. R.; Williams, P. A.; Kloprogge, J. T.; Frost, R. L. *Neues Jahrb. Mineral., Monatsh.* **2001**, *11*, 505-519.

(9) Watson, V.; Clay, H. F. *J. Oil Colour Chem. Assoc.* **1955**, *38*, 167-177.

(10) Cole, R. J. *Res. Assoc. Br. Paint, Colour Varn. Manuf.* **1955**, *10*, 1-62.

(11) Monico, L.; Van der Snickt, G.; Janssens, K.; De Nolf, W.; Miliani, C.; Dik, J.; Radepon, M.; Hendriks, E.; Geldof, M.; Cotte, M. *Anal. Chem.* **2011**, *83*, 1224-1231.

(12) Monico, L.; Janssens, K.; Miliani, C.; Brunetti, B. G.; Vagnini, M.; Vanmeert, F.; Falkenberg, G.; Abakumov, A.; Lu, Y.; Tian, H.; Verbeeck, J.; Radepon, M.; Cotte, M.; Hendriks, E.; Geldof, M.; van der Loeff, L.; Salvant, J.; Menu, M. *Anal. Chem.* **2013**, *85*, 851-859.

(13) Monico, L.; Janssens, K.; Vanmeert, F.; Cotte, M.; Brunetti, B. G.; Van der Snickt, G.; Leeuwestein, M.; Salvant Plisson, J.; Menu, M.; Miliani, C. *Anal. Chem.* **2014**, *86*, 10804-10811.

(14) Monico, L.; Van der Snickt, G.; Janssens, K.; De Nolf, W.; Miliani, C.; Verbeeck, J.; Tian, H.; Tan, H.; Dik, J.; Radepon, M.; Cotte, M. *Anal. Chem.* **2011**, *83*, 1214-1223.

(15) Munoz-Garcia, A. B.; Massaro, A.; Pavone, M. *Chem. Sci.* **2016**, *7*, 4197-4203.

(16) Amat, A.; Miliani, C.; Fantacci, S. *RSC Adv.* **2016**, *6*, 36336-36344.

(17) Li, C.-T.; Chang, H.-Y.; Li, Y.-Y.; Huang, Y.-J.; Tsai, Y.-L.; Vittal, R.; Sheng, Y.-J.; Ho, K.-C. *ACS Appl. Mater. Interfaces* **2015**, *7*, 28254-28263.

(18) Jin, Z.; Yang, M.; Chen, S.-H.; Liu, J.-H.; Li, Q.-X.; Huang, X.-J. *Anal. Chem.* **2017**, *89*, 2613-2621.

(19) Anaf, W.; Janssens, K.; De Wael, K. *Angew. Chem., Int. Ed.* **2013**, *52*, 12568-12571.

(20) Ayalew, E.; Janssens, K.; De Wael, K. *Anal. Chem.* **2016**, *88*, 1564-1569.

(21) Hohenberg, P.; Kohn, W. *Phys. Rev.* **1964**, *136*, B864-B871.

(22) Kohn, W.; Sham, L. J. *Phys. Rev.* **1965**, *140*, A1133-A1138.

(23) Blöchl, P. E. *Phys. Rev. B* **1994**, *50*, 17953-17979.

(24) Kresse, G.; Hafner, J. *Phys. Rev. B* **1993**, *47*, 558-561.

(25) Kresse, G.; Hafner, J. *J. Phys.: Condens. Matter* **1994**, *6*, 8245-8257.

(26) Kresse, G.; Furthmüller, J. *Comput. Mater. Sci.* **1996**, *6*, 15-50.

(27) Kresse, G.; Furthmüller, J. *Phys. Rev. B* **1996**, *54*, 11169-11186.

(28) Anisimov, V. I.; Zaanen, J.; Andersen, O. K. *Phys. Rev. B* **1991**, *44*, 943-954.

(29) Liechtenstein, A. I.; Anisimov, V. I.; Zaanen, J. *Phys. Rev. B* **1995**, *52*, R5467-R5470.

(30) Perdew, J. P.; Burke, K.; Ernzerhof, M. *Phys. Rev. Lett.* **1996**, *77*, 3865-3868.

(31) Perdew, J. P.; Burke, K.; Ernzerhof, M. *Phys. Rev. Lett.* **1997**, *78*, 1396-1396.

(32) Jain, A.; Ong, S. P.; Hautier, G.; Chen, W.; Richards, W. D.; Dacek, S.; Cholia, S.; Gunter, D.; Skinner, D.; Ceder, G.; Persson, K. A. *APL Mater.* **2013**, *1*, 011002-011012.

(33) Monkhorst, H. J.; Pack, J. D. *Phys. Rev. B* **1976**, *13*, 5188-5192.

(34) Hinuma, Y.; Grüneis, A.; Kresse, G.; Oba, F. *Phys. Rev. B* **2014**, *90*, 155405-155420.

(35) Schleife, A.; Fuchs, F.; Rödl, C.; Furthmüller, J.; Bechstedt, F. *Appl. Phys. Lett.* **2009**, *94*, 012104-012106.

(36) Bandiello, E.; Errandonea, D.; Martinez-Garcia, D.; Santamaria-Perez, D.; Manjón, F. J. *Phys. Rev. B* **2012**, *85*, 024108-024117.

(37) Errandonea, D.; Bandiello, E.; Segura, A.; Hamlin, J. J.; Maple, M. B.; Rodriguez-Hernandez, P.; Muñoz, A. J. *Alloys Compd.* **2014**, *587*, 14-20.

(38) Ong, S. P.; Andreussi, O.; Wu, Y.; Marzari, N.; Ceder, G. *Chem. Mater.* **2011**, *23*, 2979-2986.

(39) Tan, H.; Tian, H.; Verbeeck, J.; Monico, L.; Janssens, K.; Van Tendeloo, G. *Angew. Chem., Int. Ed.* **2013**, *52*, 11360-11363.

(40) Cepriá, G.; García-Gareta, E.; Pérez-Arantegui, J. *Electroanalysis* **2005**, *17*, 1078-1084.

(41) Sarmadian, N.; Saniz, R.; Partoens, B.; Lamoen, D.; Volety, K.; Huyberegts, G.; Paul, J. *Phys. Chem. Chem. Phys.* **2014**, *16*, 17724-17733.

(42) Sarmadian, N.; Saniz, R.; Partoens, B.; Lamoen, D. *Sci. Rep.* **2016**, *6*, 20446-20454.

(43) Monico, L.; Janssens, K.; Cotte, M.; Romani, A.; Sorace, L.; Grazia, C.; Brunetti, B. G.; Miliani, C. *J. Anal. At. Spectrom.* **2015**, *30*, 1500-1510.

(44) Reference Solar Spectral Irradiance: Air Mass 1.5 <http://rredc.nrel.gov/solar/spectra/am1.5/> (Date of access: 04/05/2016).

Table of contents graphic

